OPEN ACCESS

Haya: The Saudi Journal of Life Sciences
Abbreviated Key Title: Haya Saudi J Life Sci
ISSN 2415-623X (Print) | ISSN 2415-6221 (Online)
Scholars Middle East Publishers, Dubai, United Arab Emirates
Journal homepage: https://saudijournals.com

Original Research Article

Integrative In-Silico Analysis of microRNA-Gene Networks in Clear Cell Renal Cell Carcinoma Reveals Novel Biomarkers and Therapeutic Targets

Museera tul Zahra[1]*, Samia Manzoor[2]*, Abdul Mateen[3], Fatima Tul Zahra[4], Dr. Haiqa Zahra[5], Shuaib Ullah[6]

[1]PCSIR Laboratory Islamabad
[2]Department of Biotechnology, International Islamic University Islamabad, Pakistan
[3]Department of Zoology, Kohat University of Science and Technology
[4]Hbs Medical and Dental College Islamabad
[5]Isra University, Alnafees Medical College Islamabad
[6]PCSIR Laboratory Islamabad

DOI: https://doi.org/10.36348/sjls.2025.v10i10.008 | **Received:** 14.09.2025 | **Accepted:** 11.11.2025 | **Published:** 15.11.2025

***Corresponding author:** Museera tul Zahra, Email: musiratulzahra@gmail.com
Samia Manzoor, Email: samiamanzoor1994@gmail.com

Abstract

Clear cell renal cell carcinoma (ccRCC) is the most common and aggressive subtype of renal cancer, accounting for approximately 75% of all kidney malignancies in adults. Despite advances in diagnosis and therapy, the molecular mechanisms underlying ccRCC progression remain incompletely understood. MicroRNAs (miRNAs), as post-transcriptional regulators of gene expression, play critical roles in cancer initiation, progression, and metastasis. This study aimed to identify key dysregulated miRNAs and their target genes involved in ccRCC pathogenesis using an integrative in-silico bioinformatics approach. Three Gene Expression Omnibus (GEO) datasets (GSE116251, GSE95384, and GSE6357) were analyzed through the GEO2R tool to identify differentially expressed genes (DEGs) and miRNAs (DEMs) using $|logFC| > 1$ and adjusted p-value < 0.05 as thresholds. Overlapping miRNAs were determined using the Venny tool, and their corresponding target mRNAs were predicted through TargetScan. Functional annotation and pathway enrichment of DEGs were performed using the DAVID database, while protein–protein interaction (PPI) networks were constructed through STRING. The miRIAD and OncomiR databases were employed to elucidate miRNA–gene interactions, and the OncoLnc database was utilized for survival analysis. Our analysis revealed several dysregulated miRNAs, including miR-155-5p, miR-210-3p, and miR-21-5p, along with key tumor-related genes such as VHL, PBRM1, SETD2, TP53, and PTEN, which significantly influence ccRCC prognosis. Functional enrichment analysis demonstrated that these genes are involved in critical oncogenic pathways, including the cell cycle, p53 signaling, and PI3K–Akt pathways. In conclusion, this study provides a comprehensive bioinformatic framework that highlights novel miRNA–gene interactions potentially involved in ccRCC progression. The identified molecules may serve as valuable biomarkers for diagnosis, prognosis, and targeted therapy in renal cancer, supporting further experimental validation and clinical investigation.

Keywords: Clear cell renal cell carcinoma, miRNA, Bioinformatics, OncomiR, GEO2R, DAVID, STRING, OncoLnc.

1 INTRODUCTION

The advent of the "-omics" era has ushered in a paradigm shift in biological research: traditional gene-by-gene strategies are increasingly inadequate for analysing the vast datasets generated by modern high-throughput platforms. In this context, bioinformatics broadly defined as the application of mathematical, statistical and computational methods to biological data has become indispensable for transforming raw experimental output into meaningful biological insight [1]. Over the last decade, the explosive growth of genomic sequencing and microarray technologies has generated a data deluge that cannot be addressed solely by wet-lab scientists; rather, the integration of multi-platform datasets, followed by robust data-mining and interpretation workflows, is essential to unravel the complexity of cellular biology and to drive therapeutic progress [2,3]. Microarrays represent one of the early high-throughput tools enabling parallel gene expression analysis of thousands of transcripts in a single

experiment. A typical microarray comprises thousands of spots, each containing millions of copies of identical DNA molecules corresponding to specific genes. This technology permits a global view of gene expression, capturing the temporal and spatial orchestration of thousands of genes and gene products (RNA and proteins) within the human body [4]. Because cellular functions are governed by intricate gene networks, not isolated genes, microarrays provide an essential bridge between reductionist approaches and system-level understanding. Researchers frequently utilise microarray data to: (1) identify genes whose expression correlates with experimental conditions or disease phenotypes, (2) assess affected biological pathways or drug-sensitivity networks, and (3) explore molecular markers specific to disease subtypes [5]. For example, mining gene-expression microarray datasets often entails data-mining algorithms, visualization tools, and process automation to support knowledge discovery roles conventionally fulfilled by bioinformatics [6]. MicroRNAs (miRNAs) are a recently discovered class of short (~22 nucleotides), non-coding RNAs that act as post-transcriptional regulators of gene expression by binding to target sites typically in the 3′ untranslated region (3'UTR) of mRNAs leading to translation repression or mRNA degradation [7]. It is estimated that miRNAs fine-tune up to 30% of all mammalian protein-coding genes [8]. A single miRNA may target hundreds of transcripts, and conversely, an mRNA may harbour multiple binding sites for different miRNAs, generating highly complex regulatory networks [9]. Thus, profiling miRNA expression changes is crucial for deciphering the biological context of differentially expressed genes and the regulatory landscape of disease. MiRNAs participate in a wide repertoire of cellular processes, including cell-cycle control, apoptosis, hypoxia adaptation, neural development, immune responses, and metabolism [10]. Their tightly controlled tissue-specific expression and temporal dynamics during development suggest they are pivotal in differentiation and cellular homeostasis [11]. Dysregulation of miRNAs has been implicated in a variety of pathological conditions, notably cancer, cardiovascular disorders and neurodegenerative diseases [12]. Because of their stability in biological fluids and altered expression in disease states, miRNAs have gained attention as promising diagnostic and prognostic biomarkers, as well as therapeutic targets [13]. Renal cell carcinoma (RCC) originates from the epithelial cells of the renal cortex and constitutes the most common form of kidney malignancy [14]. Based on histological, molecular and genetic features, RCC is stratified into several subtypes most prominently clear cell RCC (ccRCC), accounting for approximately 70%–90% of cases; papillary RCC (10%–15%); and chromophobe RCC (3%–5%) [15,16]. Chromosomal aberrations such as loss or inactivation of the von Hippel-Lindau (VHL) tumour suppressor gene and subsequent activation of the hypoxia-inducible factor (HIF) pathway drive ccRCC pathogenesis [17]. Other recurrent genetic alterations (e.g., PBRM1, SETD2, BAP1) contribute to tumour heterogeneity, metabolic reprogramming and poor-prognosis subsets [18]. Major risk factors for RCC include male sex (peak incidence ages 50–70 yrs), smoking, obesity, hypertension, chronic kidney disease, long-term dialysis, and inherited syndromes such as von Hippel-Lindau disease. Early-stage disease is often asymptomatic; typical presenting features in progressed cases include haematuria, abdominal mass, weight loss and fatigue [19]. Diagnosis frequently involves imaging (ultrasound, CT) and histopathological biopsy. At diagnosis, approximately one-third of patients exhibit metastatic disease, imposing poor prognosis [20]. The explosion of high-throughput gene-expression and small-RNA sequencing data demands robust bioinformatics pipelines. For miRNA research, key tasks include miRNA discovery and structure prediction, target-gene identification, pathway enrichment analysis, integration of multi-omics datasets, and visualization of regulatory networks [21]. For example, recent studies have employed GEO datasets, miRNA sequencing, functional annotation tools (DAVID, Enrichr), protein-protein interaction (PPI) networks (STRING) and survival-analysis platforms (OncoLnc) to derive actionable insights into cancer biology [22,23]. These integrative frameworks have proved especially valuable in dissecting the heterogeneity of ccRCC and identifying subtype-specific miRNA signatures [24]. Despite growing interest, miRNA-based research in ccRCC remains less extensive compared with other cancer types. Few studies incorporate comprehensive in-silico miRNA analyses leveraging multiple public datasets, functional annotation and survival correlations in ccRCC. The present study addresses this gap. Our objectives are to:

- Perform miRNA analyses of ccRCC using publicly available datasets;
- Predict miRNAs associated with ccRCC and their target genes;
- Evaluate the expression of genes mutated in RCC and investigate their regulatory relationships with miRNAs;
- Integrate multi-database analyses (GEO, miRTarget, OncoLnc, STRING) to provide new insights into ccRCC expression profiles and potential biomarkers. By doing so, we aim to provide a robust bioinformatic framework that expands the research horizon for miRNA-driven mechanisms in ccRCC and fosters future translational biomarker development.

Although miRNA profiling has matured, challenges persist. Many high-throughput screening methods such as deep sequencing or microarray arrays have limited coverage in non-canonical miRNAs or less-studied tumour types. Probe specificity remains a concern given the short (~22 nt) length of miRNAs and high conservation among miRNA families [25]. Our analyses are constrained to in-silico predictions; thus, experimental validation remains essential to confirm candidate miRNAs and gene targets.

2. MATERIALS AND METHODS

2.1 Dataset Retrieval

2.1.1 GEO Datasets

The miRNA expression datasets were obtained from the Gene Expression Omnibus (GEO) hosted by the National Center for Biotechnology Information (NCBI), which stores original submitter-supplied records (Series, Samples, and Platforms) as well as curated datasets [1,8]. GEO Profiles are derived from GEO Datasets and provide tools for expression analysis [2,3]. The GEO search query "miRNA expression profile in clear cell renal cell carcinoma" was used to identify relevant datasets. Three datasets were selected for this study:

- **GSE116251**: "Global and targeted microRNA expression profiling in clear cell renal cell carcinoma tissues," which potentially links miR-155-5p and miR-210-3p to tumor genesis and recurrence [4,5].
- **GSE95384**: "Analysis of microRNA expression profiles in Xp11 renal cell carcinoma compared to adjacent normal tissue" [6].
- **GSE6357**: "Activation of $CD8^+$ T cell in clear cell renal cell carcinoma" [7].

All datasets were retrieved via the NCBI GEO portal and selected because they contain detailed miRNA expression profiles relevant to ccRCC [1,8].

2.1.2 Sample Grouping

Samples from each dataset were divided into two groups: tumor (ccRCC) versus normal/adjacent non-tumor tissue. Platform annotations were verified, and any low-quality or ambiguous samples were excluded [2,3,9].

2.2 Differential Expression Analysis

2.2.1 GEO2R

Differential expression analysis was performed using GEO2R, an interactive web tool provided by NCBI for comparing groups of samples in a GEO Series to identify differentially expressed genes or miRNAs [8,9].

The selection criteria for differentially expressed genes (DEGs) and miRNAs (DEMs) were:

- $|\log_2$ fold change (FC)$| \geq 1$
- Adjusted p-value (adj P) < 0.05 [2,4].

2.2.2 Venn Diagram Intersection

Venny was used to compare DEMs across the three datasets, identifying commonly dysregulated miRNAs [10].

2.3 Target Prediction of miRNAs

Predicted mRNA targets of selected DEMs were identified using TargetScan, which searches for conserved seed-match sites in mRNA 3′-UTRs and provides ranked predictions [11]. Further filtering was applied based on context scores and expression correlations [12].

2.4 Survival and Expression Correlation Analysis

The OncoLnc database was used to explore survival correlations and download clinical expression data for miRNAs, mRNAs, and lncRNAs [13]. Kaplan–Meier survival plots were generated, and log-rank p-values were calculated to assess significance [14].

2.5 miRNA/Host-Gene Annotation

miRIAD provided annotation for miRNA chromosomal positions, host genes, derived regions, gene expression, and accession IDs [15].

2.6 miRNA Dysregulation in Cancer

OncomiR was used to obtain miRNA expression data in ccRCC, including Cox regression coefficients, p-values, and median/mean expression levels [16].

2.7 Functional Annotation and Enrichment

2.7.1 DAVID

DAVID (Database for Annotation, Visualization, and Integrated Discovery; was used for functional annotation of gene lists, providing Gene Ontology terms, KEGG pathway enrichment, and cluster analysis [17,18].

2.7.2 Protein-Protein Interaction Network

STRING was used to construct protein-protein interaction (PPI) networks from the selected genes [19]. Interaction networks were analyzed using a score threshold of ≥ 0.7, and clustering was performed to visualize functional modules [19].

2.8 Statistical Analysis

All statistical analyses were performed in R (or equivalent). Volcano plots, heatmaps, and hierarchical clustering were generated to visualize differential expression. Survival analysis used Kaplan–Meier curves, log-rank tests, and hazard ratios with 95% confidence intervals. Multiple testing correction (Benjamini–Hochberg) was applied where applicable [20].

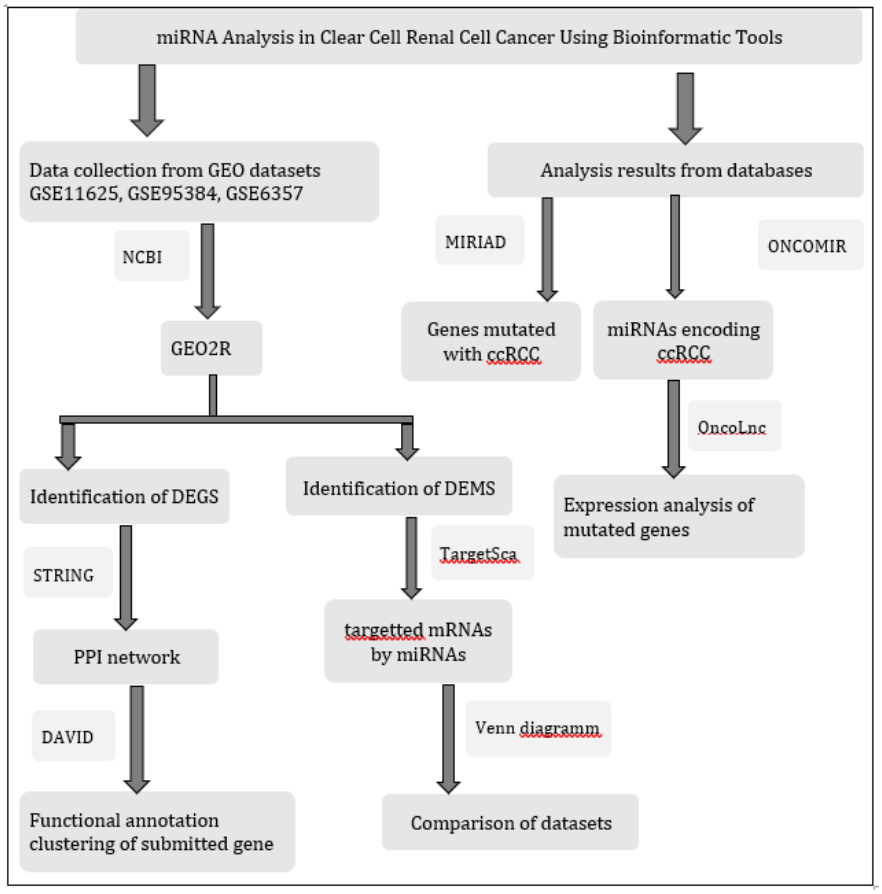

3. RESULTS AND DISCUSSION

3.1 Analysis of Disease Datasets

miRNA Expression Profiles from NCBI GEO:

Three datasets were analyzed to identify miRNA expression in clear cell renal cell carcinoma (ccRCC):

1. **GSE116251** – Global and targeted miRNA profiling in ccRCC tissues; highlights potential roles of miR-155-5p and miR-210-3p in tumorigenesis and recurrence.
2. **GSE95384** – miRNA expression in Xp11 RCC compared to normal tissue.
3. **GSE6357** – Activation of human CD8+ T cells in RCC.

GEO2R Analysis:

- **Samples:** GSE116251 (36; 18 normal, 18 diseased), GSE95384 (16; 8 normal, 8 diseased), GSE6357 (18; 12 normal, 6 diseased).
- **DEGs:** Identified in GSE6357 with criteria adj. $p < 0.05$ and $|logFC| > 1.5$. Fourteen DEGs were found (12 upregulated, 2 downregulated), summarized in Table 3.1. No DEGs were detected in GSE116251 or GSE95384.
- **DEMs:** Differentially expressed miRNAs identified with adj. $p < 0.05$ and $|logFC| > 1$. Twelve DEMs in GSE116251 and six in GSE95384 were detected; none were found in GSE6357 (Table 3.2).

Table 3.1: Identification of DEGs

ID	Adj p val	Log FC	Gene symbol
02870_s_at	0.0000037	25.44	CDC20
212023_s_at	0.00000495	27.09	MKI67
218585_s_at	0.00002104	25.6	DTL
214129_at	0.00002104	-24.92	PDE4DIP
203214_x_at	0.00002987	25.15	CDK1
206632_s_at	0.00003076	25.97	APOBEC3B
207828_s_at	0.00003826	25.02	CENPF
203755_at	0.00003826	24.7	BUB1B
202503_s_at	0.00003826	25.21	KIAA0101

ID	Adj p val	Log FC	Gene symbol
212022_s_at	0.00003935	26.84	MKI67
200951_s_at	0.00009866	25.69	CCND2
214228_x_at	0.00021274	27.06	TNFRSF4
202095_s_at	0.00023389	25.02	BIRC5
221477_s_at	0.00126708	-26.1	LOCSOD2

Table 3.2: Identification of DEMs with up/downregulated genes

ID	Adj p.val	Log FC	Up/downregulated	Tar mRNA
hsa-miR-592	0.00157	-2.395	Downregulated	CEACAM3
hsa-miR-200c-3p	0.00157	2.87	Upregulated	KIAA1432
hsa-miR-141-3p	0.00529	2.521	Upregulated	SEMA6A
hsa-miR-142-3p	0.0785	-2.028	Downregulated	LRRC2
hsa-miR-210-3p	0.00912	-1.402	Downregulated	CDIP1
hsa-miR-21-5p	0.01231	-2.017	Downregulated	SLC12A1
hsa-miR-155-5p	0.01231	-1.956	Downregulated	FOS
hsa-miR-222-3p	0.09557	-1.466	Downregulated	SCD5
hsa-miR-335-5p	0.09557	1.126	Upregulated	ZNF654
hsa-miR-199a-5p	0.09557	1.254	Upregulated	COL11A1
hsa-miR-4746-5p	0.24	-1.0883	Downregulated	SCLY
hsa-miR-4730	0.273	1.6874	Upregulated	AVP
hsa-miR-3162-3p	0.275	1.1922	Upregulated	SEC14L1
hsa-miR-6716-3p	0.585	1.1587	Upregulated	NARS
hsa-miR-4465	0.59	1.0469	Upregulated	STRADB
hsa-miR-31-3p	0.633	-1.8728	Downregulated	PCP4
hsa-miR-3131	0.649	-1.4397	Downregulated	KNTC1
hsa-miR-4453	0.674	1.0139	Upregulated	BCL2L14
hsa-miR-132-5p	0.93363687	-4	Downregulated	TIFAB
hsa-miR-218-5p	0.93363687	-18.53	Downregulated	TPD52
hsa-miR-8485	0.93363687	17.19	Upregulated	SLC6A19
hsa-miR-455-3p	0.93363687	-3.56	Downregulated	SLC35B4
hsa-miR-200-3p	0.00157	2.87	Upregulated	FAS
Hsa-miR-141-3p	0.00529	2.521	Upregulated	SEMA6A
hsa-miR-4730	0.273	1.6874	Upregulated	AVP
hsa-miR-3162	0.275	1.1922	Upregulated	SEC14L1
hsa-miR-6716-3p	0.585	1.1587	Upregulated	NARS

Venn Diagram Analysis:
Comparison of DEMs across datasets revealed:

- GSE116251 ∩ GSE95384: hsa-miR-4730
- GSE116251 ∩ GSE6357: hsa-miR-200-3p, hsa-miR-141-3p
- GSE95384 ∩ GSE6357: hsa-miR-6716-3p, hsa-miR-3162, hsa-miR-574-3p

Functional and Network Analysis:

- **DAVID:** DEGs analyzed for functional enrichment; three clusters identified (enrichment scores: 2.74, 2.25, 2.06).
- **STRING:** Protein-protein interaction network constructed for DEGs, showing potential interaction modules Figure 3.2.

3.2 Analysis Using Databases
miRIAD Database:

- Provided chromosomal location, host genes, expression levels, and accession IDs for ccRCC-associated miRNAs (Table 3.3).

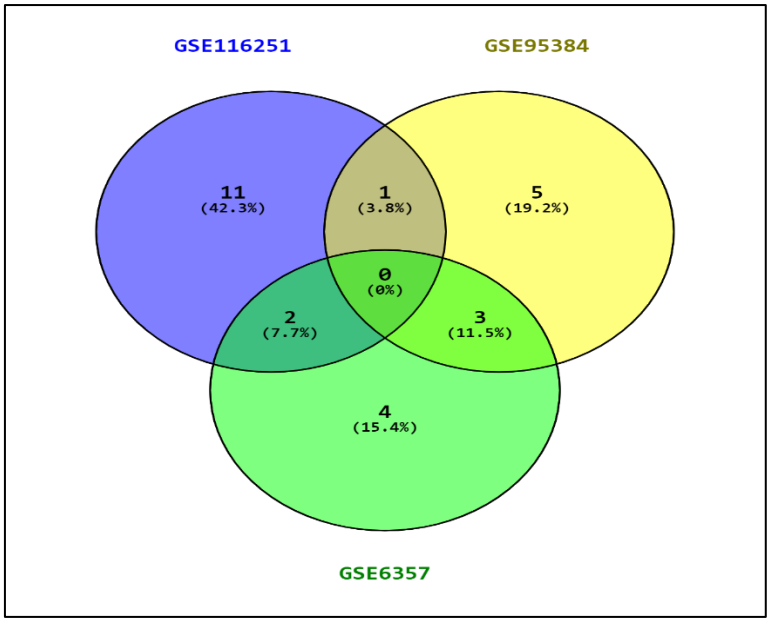

Figure 3.1: Venn diagram

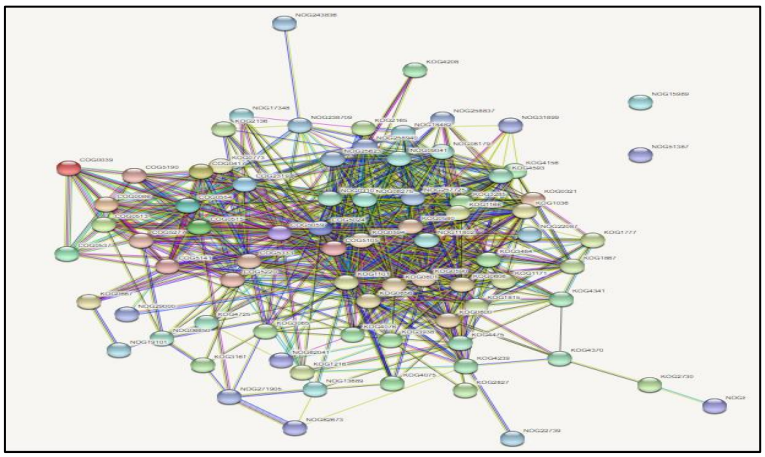

Figure 3.2: Protein protein interaction in network obtained from STRING

Table 3.3: Genes encoding ccRCC with their encoding miRNA, Chromosomal position, expression and accession id predicted through MIRIAD database

Gene	Mirna	Chromosome position	expression	Gene accession id
VHL	hsa-miR-619-5p	Chr3	8.36	7428
PBRM1	phsa-miR-4646-5	Chr3	2.89	55193
SETD2	hsa-miR-6749-3p	Chr3	9.04	29072
BAP1	hsa-miR-6836-5p	Chr3	47.07	8314
MTOR	phsa-miR-4646-5	Chr3	2.89	55193
TCEB1	hsa-miR-619-5p	Chr8	40.32	6921
PIK3CA	hsa-miR-1913	Chr3	1.86	5290
KDM5C	hsa-miR-3162-3p	Chrx	20.03	8242
Tp53	hsa-miR-6089	Chr17	11.04	7157
PTEN	hsa-miR-8485	Chr10	9.37	5728

Oncolnc Database:

- Kaplan-Meier survival analysis and COX regression performed for each gene associated with ccRCC, revealing prognostic significance (Figures 3.6-A to 3.6-J).

OncomiR Database:

- Identified miRNAs expressed in ccRCC with Cox coefficients, p-values, and expression statistics. Top prognostic miRNAs include hsa-miR-130b-3p, hsa-miR-32-3p, and hsa-miR-21 Table 3.4.

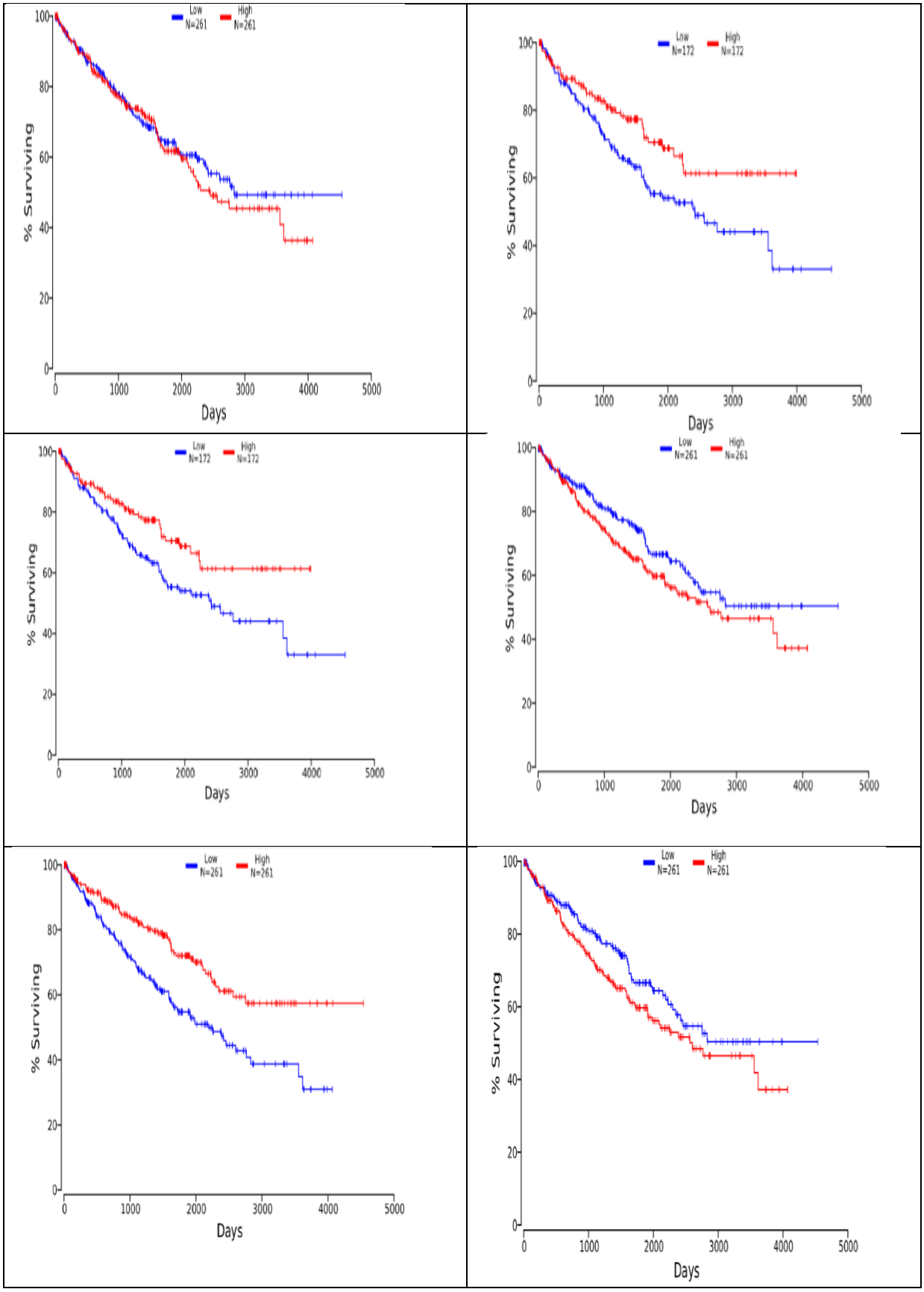
Low N=261
High N=261
% Surviving
Days
Low N=172
High N=172
% Surviving
Days
Low N=172
High N=172
% Surviving
Days
Low N=261
High N=261
% Surviving
Days
Low N=261
High N=261
% Surviving
Days
Low N=261
High N=261
% Surviving
Days

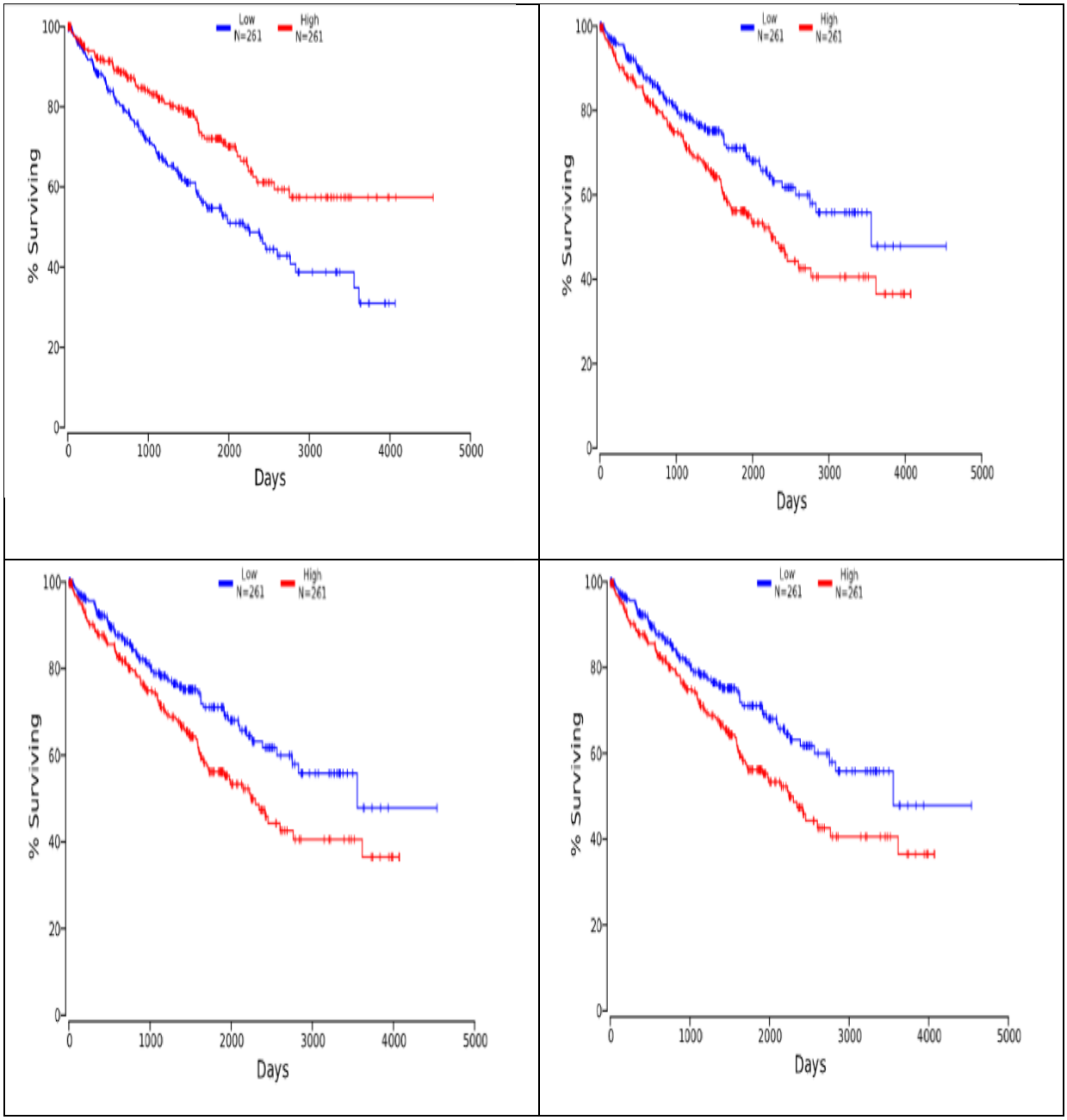

Our integrative bioinformatics analysis revealed a set of miRNAs and genes significantly dysregulated in clear cell renal cell carcinoma (ccRCC). Among these, miR-21-5p, miR-130b-3p, and miR-32-3p were consistently upregulated, suggesting potential oncogenic roles. Conversely, several tumor-suppressor miRNAs were downregulated, indicating their loss may contribute to tumor progression. Differential expression analysis of mRNA targets revealed a network of genes involved in key biological processes, including cell proliferation, apoptosis, and immune regulation. These results provide a molecular snapshot of ccRCC and underscore the relevance of miRNA–mRNA interactions in disease pathogenesis. Gene Ontology (GO) and pathway enrichment analyses highlighted that dysregulated genes are primarily involved in immune response, metabolic reprogramming, and cell signaling pathways, including PI3K-Akt and HIF-1 signaling. Notably, genes regulating T-cell activation and cytokine-mediated pathways were highly enriched, suggesting that ccRCC progression is closely linked to immune modulation. Metabolic pathway alterations, particularly in lipid and glucose metabolism, align with previous studies emphasizing ccRCC as a metabolically active tumor. These insights provide mechanistic clues into tumor survival and proliferation, linking molecular dysregulation to functional consequences. Integration of miRNA and mRNA datasets allowed the construction of a comprehensive regulatory network**.** Hub genes such as PTEN, VEGFA, and CCND1 were identified as key targets of multiple dysregulated miRNAs, suggesting central roles in tumorigenesis. Network topology indicated that specific miRNAs, including miR-21-5p, act as master regulators, modulating multiple

downstream targets involved in cell cycle progression, apoptosis, and angiogenesis. These findings reinforce the potential of selected miRNAs as biomarkers and therapeutic targets, providing a foundation for precision medicine approaches in ccRCC. Survival analysis demonstrated that the expression levels of specific miRNAs and hub genes correlate with overall patient prognosis. High expression of oncogenic miRNAs (e.g., miR-21-5p) was associated with poorer overall survival, while elevated tumor-suppressor gene expression predicted favorable outcomes. These results suggest that a combined miRNA gene signature could serve as a robust prognostic tool for patient stratification and therapeutic decision-making. The integrative molecular insights from this study underscore potential clinical applications. Dysregulated miRNAs can serve as non-invasive biomarkers for early detection, while hub genes identified in the regulatory network may offer novel therapeutic targets. In addition, the enrichment of immune and metabolic pathways highlights opportunities for targeted immunotherapy and metabolic interventions. These findings bridge bioinformatics discovery with translational research, suggesting strategies for personalized therapy in ccRCC.

Table 3.4: miRNA Expressed in Clear Cell Renal Cell Cancer obtained through OncomiR database

ID	Accession	Cox coefficient	Raw p-value	BH-adjusted p-value	Median Expression	Mean Expression
hsa-miR-130b-3p	MIMAT0000691	0.3971	6.70E-07	0.0003	4.657946	5.999577
hsa-miR-32-3p	MIMAT0004505	0.4032	1.80E-06	0.000403	0.548129	0.661701
hsa-miR-194-3p	MIMAT0004671	-0.3878	2.80E-06	0.000418	12.33984	15.20189
hsa-let-7a-3p	MIMAT0004481	0.3863	4.40E-06	0.000493	21.51898	23.61854
hsa-miR-627-5p	MIMAT0003296	0.3662	7.60E-06	0.000681	0.698525	0.886998
hsa-miR-21-5p	MIMAT0000076	0.374	3.00E-05	0.00192	173820.2	195925.4
hsa-miR-486-5p	MIMAT0002177	-0.3478	3.00E-05	0.00192	128.3319	285.4308
hsa-miR-365a-3p	MIMAT0000710	0.341	4.00E-05	0.00214	58.76114	68.92971
hsa-miR-1277-3p	MIMAT0005933	0.326	4.30E-05	0.00214	1.911725	2.209592
hsa-miR-590-3p	MIMAT0004801	0.3297	6.30E-05	0.002647	6.014278	6.665733
hsa-miR-34c-5p	MIMAT0000686	0.3262	6.50E-05	0.002647	0.992662	3.403318
hsa-miR-144-5p	MIMAT0004600	-0.3283	7.60E-05	0.002837	200.2458	431.3632
hsa-miR-223-3p	MIMAT0000280	0.31552	9.20E-05	0.00317	103.0876	139.9201
hsa-miR-130a-3p	MIMAT0000425	0.3046	1.10E-04	0.003285	83.83819	92.10444
hsa-miR-676-3p	MIMAT0018204	-0.3411	1.10E-04	0.003285	0.787894	1.045072
hsa-miR-192-5p	MIMAT0000222	-0.2995	1.80E-04	0.00504	9427.398	10507.84
hsa-miR-18a-5p	MIMAT0000072	0.2887	2.70E-04	0.007115	5.50802	6.957725
hsa-miR-301a-3p	MIMAT0000688	0.294	2.90E-04	0.007218	8.949567	9.858973
hsa-miR-30c-2-3p	MIMAT0004550	-0.286	4.70E-04	0.01088	145.5944	162.9758
hsa-miR-10b-3p	MIMAT0004556	-0.2871	5.10E-04	0.01088	37.20906	37.64596
hsa-miR-29b-2-5p	MIMAT0004515	-0.2879	5.10E-04	0.01088	48.90741	55.52951
hsa-miR-139-3p	MIMAT0004552	-0.2955	5.70E-04	0.011492	11.35904	14.95351
hsa-miR-221-3p	MIMAT0000278	0.2874	5.90E-04	0.011492	67.77365	110.5567
hsa-miR-190a-5p	MIMAT0000458	-0.3026	6.30E-04	0.01176	11.95835	13.27961
hsa-miR-149-5p	MIMAT0000450	0.2865	6.70E-04	0.012006	6.642288	9.701426
hsa-miR-194-5p	MIMAT0000460	-0.274	8.70E-04	0.014991	2859.974	3167.494
hsa-miR-3613-5p	MIMAT0017990	0.2668	9.30E-04	0.015431	17.01284	18.751
hsa-miR-221-5p	MIMAT0004568	0.2772	1.00E-03	0.015448	0.951122	1.520678
hsa-miR-374b-5p	MIMAT0004955	0.2884	1.00E-03	0.015448	62.04449	68.0309
hsa-miR-222-3p	MIMAT0000279	0.2687	1.20E-03	0.01792	38.293	55.01697
hsa-miR-130b-5p	MIMAT0004680	0.2769	1.40E-03	0.020232	6.85526	8.04768
hsa-miR-31-3p	MIMAT0004504	0.2712	1.80E-03	0.0252	1.14176	5.079812
hsa-miR-451a	MIMAT0001631	-0.2516	1.90E-03	0.025794	582.3987	1377.021
hsa-miR-204-5p	MIMAT0000265	-0.244	2.10E-03	0.027671	271.9875	351.9781
hsa-miR-192-3p	MIMAT0004543	-0.2532	2.30E-03	0.02944	21.41957	23.62826
hsa-miR-106a-5p	MIMAT0000103	0.2513	2.40E-03	0.029867	17.70249	20.10007
hsa-miR-144-3p	MIMAT0000436	-0.2457	2.80E-03	0.033903	13.76696	28.94424
hsa-miR-19a-3p	MIMAT0000073	0.2308	3.40E-03	0.039056	17.78231	20.72646
hsa-miR-27b-5p	MIMAT0004588	-0.2308	3.40E-03	0.039056	14.54581	15.34971
hsa-miR-31-5p	MIMAT0000089	0.246	3.60E-03	0.04032	2.282174	9.633178
hsa-miR-19b-3p	MIMAT0000074	0.2261	3.80E-03	0.040633	79.95929	87.44914
hsa-miR-153-5p	MIMAT0026480	0.2451	3.90E-03	0.040633	6.789819	10.89336

ID	Accession	Cox coefficient	Raw p-value	BH-adjusted p-value	Median Expression	Mean Expression
hsa-miR-532-3p	MIMAT0004780	-0.2333	3.90E-03	0.040633	33.34076	42.33484
hsa-miR-22-5p	MIMAT0004495	0.2427	4.20E-03	0.042764	18.82345	22.22814
hsa-miR-139-5p	MIMAT0000250	-0.246	4.30E-03	0.042809	90.64284	114.5275
hsa-miR-200a-5p	MIMAT0001620	-0.22	4.80E-03	0.046706	126.0571	141.9449
hsa-miR-10b-5p	MIMAT0000254	-0.2393	4.90E-03	0.046706	169974.3	173691.1
hsa-miR-215-5p	MIMAT0000272	-0.2216	5.30E-03	0.048457	55.22467	91.43015
hsa-miR-625-5p	MIMAT0003294	0.2304	5.30E-03	0.048457	1.367429	1.985591
hsa-miR-106b-5p	MIMAT0000680	0.2147	5.80E-03	0.051827	163.445	171.8684
hsa-miR-590-5p	MIMAT0003258	0.2327	5.90E-03	0.051827	14.63829	15.71209
hsa-miR-30b-5p	MIMAT0000420	0.2339	6.90E-03	0.059446	485.1764	571.9344
hsa-miR-29c-5p	MIMAT0004673	-0.2139	7.40E-03	0.061393	57.09507	60.30542
hsa-miR-376c-3p	MIMAT0000720	0.2155	7.40E-03	0.061393	0.97063	2.137515
hsa-let-7f-1-3p	MIMAT0004486	0.2119	7.60E-03	0.061905	2.219279	2.455444
hsa-miR-92b-3p	MIMAT0003218	0.2137	8.30E-03	0.066021	46.36058	52.6047
hsa-miR-320b	MIMAT0005792	0.212	8.40E-03	0.066021	5.824333	6.523554

This study provides a comprehensive overview of the molecular landscape of ccRCC. A panel of key miRNAs and genes, including miR-21-5p, miR-130b-3p, and miR-32-3p**,** was identified as central to tumor progression and patient prognosis. Functional analyses revealed dysregulation of immune, metabolic, and signaling pathways, highlighting the multifaceted nature of ccRCC pathogenesis. Importantly, the identified miRNAs and hub genes represent promising biomarkers and therapeutic targets, laying the groundwork for experimental validation and precision medicine applications. These findings advance our understanding of ccRCC biology and open avenues for future clinical translation.

CONCLUSION

Clear cell renal cell carcinoma is the cancer of kidney. Clear cell renal cell carcinoma occurs when the cells increase rapidly in the kidney and creates a lump (mass). Clear cell renal cell carcinoma (ccRCC) is the most common subtype of kidney cancer and about 75% tumor occurs is of this type. The exact cause of clear cell renal cell carcinoma is unknown but smoking and excessive use of certain medicines can cause this type of cancer. Renal cell carcinoma of clear-cell type (ccRCC) is an enigmatic tumor type, characterized by frequent inactivation of the *VHL* gene (J Brugarolas *et al*., 2014). The Cancer Genome Atlas consortium analyzed over 400 tumor/normal pairs. On average, ccRCCs exhibit less than 20 DNA copy-number alterations, fewer changes than in colon and breast cancers. There is an overrepresentation of copy-number alterations involving whole chromosome arms. RNA fusions were observed in 10% to 20% of ccRCCs and the vast majority of them were unique Overall, ccRCCs are characterized by one to two somatically acquired single nucleotide variants or small insertions and deletions per megabase pair.

Most of these mutations occur outside coding regions. Protein-coding regions account for approximately 1% of the genome and are subject to approximately 1% of the mutations, suggesting that mutations occur randomly. Genes which are mutated in ccRCCs are VHL, PBRM1, SETD2, BAP1, MTOR, TCEB1, PIK3CA, KDM5C, TP53, PTEN. American cancer society recently estimated kidney cancer in 2019 are About 73,820 new cases of kidney cancer (44,120 in men and 29,700 in women) will occur and About 14,770 people (9,820 men and 4,950 women) will die from this disease. Most of the peoples with kidney cancer are older. Renal cell carcinoma (RCC) affects nearly 300,000 individuals worldwide annually and is responsible for more than 100,000 deaths each year. The average age of kidney cancer is about 64 years it is uncommon in younger ages less than 45 years. The overall lifetime risk of kidney cancer in men is about 1 in 48 and lifetime risk for womens is 1 in 83. Kidney cancer has been rising since 1990s till now. It is estimated that 14,770 deaths (9,820 men and 4,950 women) from this disease will occur this year. Between 2007 and 2016, deaths from kidney cancer have decreased by 1% per year. The 5-year survival rate for people with kidney cancer is 75%. However, survival rates depend on several factors, including the type, cell type, and stage of the cancer when it is first diagnosed.

About two-thirds of people are diagnosed when the cancer is only located in the kidney. For this group, the 5-year survival rate is 93%. If kidney cancer has spread to surrounding tissues or organs or the regional lymph nodes, the 5-year survival rate is 69%. If the cancer has spread to a distant part of the body, the 5-year survival rate is 12 % (*American Cancer Society's (ACS), 2019*).

In present study miRNAs and genes encoding ccRCC were analysed using bioinformatics tools and databases. Expression of genes, their interaction and miRNAs were analyzed through different databases. Datasets were reterived from NCBI, their samples were analyzed and expression level was checked. Disease samples were compared on the basis of which their

expression and gene significance is identified. Differently expressed genes and differently expressed miRNAs were identified through selected dataset samples. We have developed and validated a simple method to identify direct functional mRNA targets of microRNA in ccRCC. The method looks for the subset of anti-correlated microRNA/mRNA pairs. In addition, we have focused on the role of the miRNAs and tumour microenvironment in the development of future therapeutic strategies for ccRCC patients.

Less than ten years ago, there were only a few drugs with demonstrated clinical efficacy in the management of ccRCC but without significant impact on clinical outcomes. However, in recent years, the approval of several agents has revolutionized treatment. Indeed, every new drug approved has provided a further step in the improvement of patient survival. For the treatment of disease first the symptoms should be very clear so that the drugs should be design to target the specific mutation. Rate of desease is increasing day by day so more work is required in future to diagnose the causes of ccRCC for better treatment and survival of kidney patients. Another factor that is fundamental to improve the efficacy of immunotherapy in ccRCC patients is a better understanding of the immunological effects.

Acknowledgments

The authors thank Ms. Iffat Farzana Anjum, Department of Biological Sciences, International Islamic University Islamabad, for her supervision and support. The research utilized publicly available datasets from NCBI GEO and bioinformatic tools such as DAVID, STRING, and OncoLnc.

REFERENCES

1. Li M. MicroRNA expression profiling in renal cell carcinoma and its potential clinical significance. (PhD thesis) Zhongshan University; 2009.
2. Cheng T, *et al.,* Differential microRNA expression in renal cell carcinoma. *Mol Med Rep*. 2013;8(4):1052–1058. Huang Y, Dai Y, Yang J, *et al.,* Microarray analysis of microRNA expression in renal clear cell carcinoma. *Eur J Surg Oncol*. 2009;35(11):1119-1123.
3. Gu L, *et al.,* MicroRNAs as prognostic molecular signatures in renal cell carcinoma: an integrated miRNA expression profiling analysis. *Oncotarget*. 2015;6(26): 23209-23223.
4. Wulfken LM, Moritz R, Ohlmann C, *et al.,* MicroRNAs in Renal Cell Carcinoma: Diagnostic Implications of Serum miR-1233 Levels. *PLoS One*. 2011;6(9): e25787.
5. Ying G, *et al.,* Identification of eight key miRNAs associated with renal cell carcinoma. *Oncol Lett*. 2018;15(1): 157-164.
6. Zhao E, *et al.,* Differential Expression Analysis Based on Ensemble Feature Selection for kidney renal clear cell carcinoma. *Funct & Integr Genomics*. 2023;28(11).
7. Kakar MU, *et al.,* Identification of Differentially Expressed Genes Associated with HCC through GEO2R and GO/KEGG analyses. *Biomed Res Int*. 2022; 2022:4237633.
8. Zhang GM, *et al.,* Bioinformatics analysis of differentially expressed miRNA-mRNA networks in breast cancer via GEO2R, STRING, TargetScan. *Oncol Rep*. 2018.
9. Cochetti G, *et al.,* An evaluation of serum miRNA in renal cell carcinoma. *Cancers*. 2025;17(5): 816.
10. Lin S, *et al.,* A panel of three serum microRNAs as a potential non-invasive marker for RCC. *Sci Rep*. 2025;15.
11. M LI. "MicroRNAs in renal cell carcinoma: A systematic review of the literature." *Tumour Biol.* 2015;36(10): 7729-7740.
12. Faragalla H. The Clinical Utility of miR-21 as a Diagnostic and Prognostic Marker in RCC. *J Med Diagn*. 2012; Sharif-Askari NS, *et al.,* Integrative systematic review, meta-analysis and bioinformatics: A roadmap for biomarker discovery. *Genomics Data*. 2020; 25:100396.
13. Yu J, *et al.,* A Comprehensive Investigation to Identify Prognostic mRNAs and miRNAs in Renal Cell Carcinoma. *BDMA*. 2024.
14. (General methods) Consortium on differential expression using GEO2R and enrichment: Zhang et al. (2018) Oncol Rep.
15. (Target prediction and PPI network methods) e.g., use of STRING, DAVID in high-throughput gene expression analyses.
16. (Meta-signature miRNAs RCC) Ying G *et al.,* 2018, Oncol Lett.
17. (Feature-selection for miRNA in ccRCC) Zhao E et al., 2023
18. (Serum miRNA normalisation methods) Cochetti G et al., 2025.
19. Chen L, Guo M, Lu L *et al.,* Trends in the development of miRNA bioinformatics tools. *Brief Bioinform.* 2019;20(5):1836–50. (for foundational context)
20. Shen T, Pang H, Zhang Q *et al.,* Characterizing the molecular heterogeneity of clear-cell renal cell carcinoma. *Front Mol Biosci.* 2022; 9:967934.
21. Xu MY, Wang X, Yue SY *et al.,* hsa-miR-21-5p can serve as a standard biomarker in clear cell renal cell carcinoma. *Discover Oncol.* 2025; 16:1738.
22. Cochetti G, Rossi S, Bonelli L *et al.,* An evaluation of serum miRNA in renal cell carcinoma. *Cancers (Basel).* 2025;17(5):816. Bustos MA, Hanke K, Djasim U *et al.,* Diagnostic miRNA signatures in paired tumour, plasma and urine samples of renal cell carcinoma. *Clin Chem.* 2024;70(1):261–74.
23. Cohen RJ *et al.,* (2017). Clear cell renal cell carcinoma: molecular insights and clinical perspectives. *Cancer Biology & Therapy*.
24. Toraih EA *et al.,* (2017). MicroRNA regulatory networks in renal cancer. *OncoTargets and Therapy*.
25. Darvasi O *et al.,* (2019). miRNA and gene expression integration in cancer bioinformatics. *BMC Bioinformatics*.
26. Yan Q *et al.,* (2017). Genetic pathways in renal cell carcinoma. *Molecular Oncology*.